



## Study of chemical composition of precipitation at an alpine site and a rural site in the Urumqi River Valley, Eastern Tien Shan, China

Zhongping Zhao <sup>a,b,c</sup>, Lide Tian <sup>a,\*</sup>, Emily Fischer <sup>d</sup>, Zhongqin Li <sup>b</sup>, Keqin Jiao <sup>b</sup>

<sup>a</sup> Laboratory of Land Surface Processes Monitoring, Institute of Tibetan Plateau Research, Chinese Academy of Sciences, Beijing, China

<sup>b</sup> Tien Shan Glaciological Station, Cold and Arid Regions Environmental and Engineering Research Institute, Chinese Academy of Sciences, Lanzhou, China

<sup>c</sup> Graduate School of Chinese Academy of Sciences, Beijing, China

<sup>d</sup> Department of Atmospheric sciences, University of Washington, Seattle, Washington, USA

### ARTICLE INFO

#### Article history:

Received 5 May 2008

Received in revised form 6 August 2008

Accepted 8 August 2008

#### Keywords:

Precipitation chemistry

Seasonal variability

Deposition fluxes

Urumqi River Valley

### ABSTRACT

We report on a 1-year continuous precipitation sampling record from an alpine site and a rural site in the Urumqi River Valley, East Tien Shan, China. The 128 samples, collected from April 2003 to February 2004, at two sites were analyzed for the major inorganic ions, pH, electrical conductivity and insoluble microparticles. The precipitation was typically alkaline with a volume-weighted mean pH of 6.99 and 7.27 at the alpine site and the rural site, respectively.  $\text{Ca}^{2+}$  was the dominant cation, and  $\text{SO}_4^{2-}$  was the dominant anion. The precipitation chemistry in this region was mainly controlled by regional Asian dust storms, local dust and anthropogenic activities. The relative impact of anthropogenic activities, specifically uncontrolled coal combustion, was larger at the rural site compared to the alpine monitoring site.

© 2008 Published by Elsevier Ltd.

### 1. Introduction

Many species of gases and aerosols from natural (crustal, biogenic, marine) and anthropogenic sources can be incorporated into raindrops or snowflakes during precipitation events. Thus information about atmospheric constituents can be inferred through the analysis of the chemical composition of precipitation. Knowledge of the chemical composition of precipitation can also provide information on the effect of regional and local pollution on the eco-system health.

In recent years, snowpack and aerosol chemistry have been studied in eastern Tien Shan (Wake et al., 1992; Williams et al., 1992; Sun et al., 1998; Jiang et al., 2002; Lee et al., 2003; Li et al., 2006; Zhao et al., 2006). However, published research on precipitation chemistry is still scarce for this region, especially in the Urumqi River Valley. In this study precipitation samples were collected at two stations

in the Urumqi River Valley, eastern Tien Shan. The base station (BS) ( $43^\circ 12' \text{N}$ ,  $87^\circ 07' \text{E}$ , 2119 m. a.s.l.), lies within a rural area, and the alpine station (AS) ( $43^\circ 06' \text{N}$ ,  $86^\circ 50' \text{E}$ , 3551 m. a.s.l.), lies within an alpine area. Meteorological data were collected at both stations including wet and dry bulb temperature, wind speed, wind direction, and precipitation.

In this work, we present the precipitation chemistry data from these two stations in the Urumqi River Valley for the period April 2003–February 2004. The data is used to identify the potential anthropogenic and natural impacts on the chemical composition of precipitation in this region. The seasonal variability and spatial trends of the precipitation chemistry and deposition fluxes are also discussed.

### 2. Study area

The Urumqi River Valley is surrounded by vast desert areas (Fig. 1): the Taklimakan Desert to the south, Gurbantunggut Desert to the north, and the Gobi Desert to the east. Evergreen vegetation exists between 1600 and

\* Corresponding author. Tel.: +86 10 62849390; fax: +86 10 62849886.  
E-mail address: [ldt@itpcas.ac.cn](mailto:ldt@itpcas.ac.cn) (L. Tian).

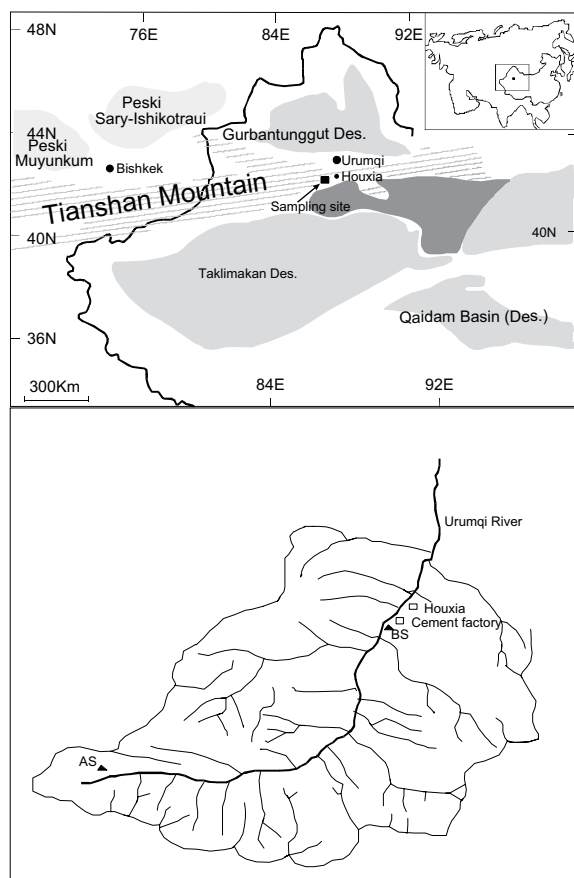


Fig. 1. Sketch map showing the sampling area and its surrounding deserts that are assumed to affect the atmospheric environment of the surveyed area.

3400 m. a.s.l in the mountains. The westerly circulation prevails across these high mountains throughout the year. Most precipitation in the Urumqi River Valley occurs during the summer months from June to August. The average annual precipitation is around 450 mm, of which about 85% occurs during summer months. The precipitation record for AS is presented in Fig. 2. The record of

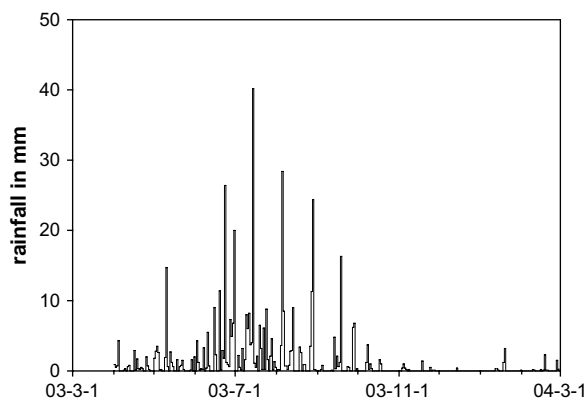


Fig. 2. Precipitation observed at AS during the sampling period.

precipitation at BS shows similar seasonal variability. Due to differences in elevation, the mean annual air temperature at BS is warmer than at AS, 1.4 °C and –4.5 °C, respectively.

There are several local industrial activities and population centers that impact the measurement sites. Urumqi, the provincial capital of Xinjiang Uygur Autonomous Region, China, with more than two million inhabitants, is 105 km to the northeast of AS and 63 km from BS. Urumqi has been ranked as one of the most severely polluted cities worldwide by several recent studies (Li et al., 2007; Mantimin and Meixner, 2007). Houxia (population: twenty thousands), which has two coal-fired power generation plants, a coal powered cement factory and various other factories, lies 8 km away from BS and 50 km from AS. The cement factory is located outside of Houxia, approximately 3 km away from BS. Fly ash and other emissions are not controlled at the power plants or at the cement factory. The output of cement plant is about three hundred tons per day. Local inhabitants primarily use coal for heating and cooking. A northeasterly valley wind prevails from March through September (Zhang et al., 1994), transporting local pollutants to the sampling sites.

### 3. Sampling and analysis

A total of 128 precipitation samples (63 at BS and 65 at AS) were collected during the investigation period. Rain samples were collected in polyethylene bottles through funnels (14 cm diameter.), while snow samples were collected in polyethylene containers (50 × 50 × 50 cm). Sampling collectors were placed on the rooftop of the buildings (about 8–10 m from ground level, and 1 m from the floor of the roof) away from surface soil and any specific emission source. Before and after each sampling, the entire collection and storage equipment were thoroughly washed and rinsed several times with de-ionized water (18.0 MQ cm quality) and then dried in a class of 100 clean bench. To prevent and minimize any possible contamination from dry deposition, the collection surface was exposed just prior to the onset of the precipitation event. A sampling event is defined as the sample collected from the onset until the end of a given precipitation event. There were 63 and 65 precipitation events sampled at BS and AS, respectively.

Electrical conductivity (EC) and pH were measured immediately after the rain event ended. Snow samples were melted at room temperature and EC and pH were measured as soon as possible. A pH meter (PHJS-4A) with a glass electrode was used for the pH measurements. The pH meter was calibrated before each measurement by using standard buffer solutions with pH of 6.86 and 9.18, respectively. The measurement resolution was 0.01 pH unit. The EC measurement was made by using a digital conductivity meter with temperature compensation (DDSJ-308A). After that samples were poured into small polyethylene bottles from the collectors as soon as possible. The samples were frozen for a period of 60 days until they were transported to the State Key Laboratory of Cryosphere and Science for chemical analysis.

In addition, aerosol sampling (TSP) was conducted at AS during this period. These aerosol samples collected for 1

day every 7 days. Detailed methods have been described by Zhao et al. (2006). We present a short summary here. Zefluor™ Teflon filters (2 µm pore size, 47 mm diameter, Gelman sciences) were used in the sampling at AS. The filters were placed facing downwards in a cylindrical polyethylene protective cover. The air was drawn by 12 V pump powered by a combination of solar cells and storage batteries. The volume of air sampled was measured by an in-line flow meter and the measured volumes were converted to standard cubic meters (scm) (0 °C, and 101.325 hPa) using ambient temperature and pressure. The flow rate was 1.27 scm h<sup>-1</sup> (+ standard deviation), sufficient to assure that the collection efficiency for particles as 0.035 µm is greater than 97% (Liu et al., 1984). The aerosol samples and blank filters were wetted with 0.2 ml ethanol, and the soluble components were then extracted with 25 ml aliquots of deionized Milli-Q water. Major ion concentrations in the aqueous extracts were determined by ion chromatography using Dionex 320 ion chromatograph.

Precipitation samples were analyzed for the major water soluble ions (Cl<sup>-</sup>, NO<sub>3</sub><sup>-</sup>, SO<sub>4</sub><sup>2-</sup>, Na<sup>+</sup>, NH<sub>4</sub><sup>+</sup>, K<sup>+</sup>, Mg<sup>2+</sup>, Ca<sup>2+</sup>) and insoluble microparticles. Ion concentrations in precipitation and aerosol samples were determined by ion chromatography (Dionex 320). Cations were analyzed using a CS12 column, 15 mM MSA eluent and CAES suppresser and the anions were quantified using an AS11-HC column, 15 mM NaOH eluent and ASRS suppresser. Certified reference materials (CRM) were used to ensure accuracy and precision (National Research Center of CRM, China). Concentrations and size distributions of insoluble microparticles in precipitation samples were analyzed by an AccuSizer 780A (0.5–400 µm measurement range with an uncertainty less than 5%). These methods had been described in detail by Zhao and Li (2004) and Li et al. (2006).

## 4. Results and discussion

### 4.1. Bicarbonate and ion balance

The cation excess  $\Delta C$  (total cation equivalents minus total anion equivalents) for BS and AS samples averaged 235.4 and 161.5 µeq. L<sup>-1</sup>. The large ionic imbalances can be attributed to the carbonate (CO<sub>3</sub><sup>2-</sup>) and bicarbonate (HCO<sub>3</sub><sup>-</sup>) ions in the precipitation. Previous work revealed a linear regression between the calcium ion (Ca<sup>2+</sup>) and  $\Delta C$  ( $R = 0.98$ ,  $N = 45$ ,  $p < 0.01$ ) in the snow, suggesting that the  $\Delta C$  represented primarily the CO<sub>3</sub><sup>2-</sup>/HCO<sub>3</sub><sup>-</sup> (Wake et al., 1992; Williams et al., 1992; Li et al., 2006). The cation excess involves the carbonate component of the dust and the CO<sub>2</sub>–CO<sub>3</sub><sup>2-</sup> equilibrium. Since no direct measurements of HCO<sub>3</sub><sup>-</sup> were available, the concentration of HCO<sub>3</sub><sup>-</sup> was estimated from the theoretical relationship between pH and HCO<sub>3</sub><sup>-</sup> (Parashar et al., 1996; Momin et al., 2005; Tiwari et al., 2007). According to this relationship, when the pH of a sample is above 5.6 and the sample is in equilibrium with atmospheric carbon dioxide pressure, the concentration of HCO<sub>3</sub><sup>-</sup> is given as  $[HCO_3^-] = 10^{-11.2 + \text{pH}}$ , with HCO<sub>3</sub><sup>-</sup> concentration in mol L<sup>-1</sup>. Estimated average values of HCO<sub>3</sub><sup>-</sup> at AS and BS were 61.7 and 117.5 µeq. L<sup>-1</sup>, compared with the cation excess  $\Delta C$  (total cation equivalents minus total

anion equivalents) for AS and BS samples averaged 161.5 and 235.4 µeq. L<sup>-1</sup>. It seems that the precipitation at both sites is heavily influence by dissolved CO<sub>2</sub>. And concentration of HCO<sub>3</sub><sup>-</sup> at AS is mainly dominated by mineral aerosols (CaCO<sub>3</sub>), while at BS is dominated by both mineral aerosols (CaCO<sub>3</sub>) and dissolved atmospheric CO<sub>2</sub>.

### 4.2. Variations of pH and EC

The pH of precipitation samples at BS ranged from 6.8 to 8.2 with a volume-weighted mean of 7.27, compared to 6.86 at Urumqi. All the individual precipitation samples had a pH value higher than 5.6, which is the pH of unpolluted water equilibrated with atmospheric CO<sub>2</sub>. Approximately 90% of the precipitation samples had a pH < 8.0. We hypothesize that this reflects the large input of alkaline species into the precipitation.

At AS the volume-weighted mean pH was 6.99, with individual precipitation samples ranging from 5.67 to 7.99, slightly more acidic than BS. Only one sample (26 April 2003) had a pH value below 6.0. This sample also had lower Ca<sup>2+</sup>, Mg<sup>2+</sup> and insoluble microparticles numbers compared to other precipitation events.

The EC of precipitation is mainly attributed to the total ionic content of the water. At BS the EC values of the precipitation samples ranged from 9.77 to 173.9 µS cm<sup>-1</sup>, with a volume-weighted mean of 35.51 µS cm<sup>-1</sup>, compared to 91.04 µS cm<sup>-1</sup> at Urumqi. At AS the volume-weighted mean EC was 26.98 µS cm<sup>-1</sup>, with individual precipitation samples ranging from 3.66 to 160.6 µS cm<sup>-1</sup>. The averaged EC at AS was almost twice than that of the precipitation (14.58 µS cm<sup>-1</sup>) at Mt. Waliguan (Tang et al., 2000), a land-based Global Atmospheric Watch (GAW) base station, located at the northeastern part of the Tibetan Plateau (36°17'N, 100°54'E, 3816 m. a.s.l.).

### 4.3. Soluble ionic compositions of precipitation

Arithmetic mean soluble species in precipitation are listed in Tables 1 and 2. At both sites, Ca<sup>2+</sup> was the dominant cation, and sulfate (SO<sub>4</sub><sup>2-</sup>) was the dominant anion. Although the ion concentrations showed large variations around their mean values, notably higher concentrations of SO<sub>4</sub><sup>2-</sup>, nitrate (NO<sub>3</sub><sup>-</sup>) and Mg<sup>2+</sup> were measured at BS compared to AS. The five major ions, Ca<sup>2+</sup>, SO<sub>4</sub><sup>2-</sup>, Mg<sup>2+</sup>, NH<sub>4</sub><sup>+</sup>, and NO<sub>3</sub><sup>-</sup>, accounted for 94.1% of the mean ionic content of the precipitation samples at BS. Especially Ca<sup>2+</sup>, accounted for 62.6% of the total ionic load. At AS, the Ca<sup>2+</sup> concentration of precipitation samples was 220.31 µeq. L<sup>-1</sup>, lower than at BS, but also a dominant ion.

**Table 1**  
Arithmetic mean soluble species in precipitation at AS (µeq. L<sup>-1</sup>).

Ion	Cl <sup>-</sup>	SO <sub>4</sub> <sup>2-</sup>	NO <sub>3</sub> <sup>-</sup>	Na <sup>+</sup>	NH <sub>4</sub> <sup>+</sup>	K <sup>+</sup>	Mg <sup>2+</sup>	Ca <sup>2+</sup>
Mean	20.95	75.46	14.11	28.89	28.77	4.62	25.97	220.31
Maximum	266.73	413.6	80.75	261.5	120.89	26.94	131.65	1150.51
Minimum	1.52	3.21	nd	1.47	nd	0.39	1.12	6.17
Standard deviation	38.7	70.51	13.79	43.03	19.81	3.89	28.54	235.62

nd means not detected.

**Table 2**  
Arithmetic mean soluble species in precipitation at BS ( $\mu\text{eq. L}^{-1}$ ).

Ion	Cl <sup>-</sup>	SO <sub>4</sub> <sup>2-</sup>	NO <sub>3</sub> <sup>-</sup>	Na <sup>+</sup>	NH <sub>4</sub> <sup>+</sup>	K <sup>+</sup>	Mg <sup>2+</sup>	Ca <sup>2+</sup>
Mean	15.89	106.86	31.72	16.3	23.21	8.24	56.07	432.15
Maximum	75.68	457.76	405.3	54.5	79.17	40.27	226.89	1624.74
Minimum	1.87	9.0	nd	0.92	nd	0.92	4.39	43.18
Standard deviation	15.47	97.22	58.63	14.44	18.63	7.8	46.86	380.82

nd means not detected.

To facilitate a discussion of regional variations in precipitation chemistry, the volume-weighted-mean values of major inorganic ions in precipitation in north China are listed in Table 3. AS had higher concentrations of all species (except for NH<sub>4</sub><sup>+</sup>) than Waliguan. Although Waliguan and AS are both located in remote areas, there are several key differences in their immediate surroundings and seasonal climates. AS is closer than Waliguan to large deserts and it is also closer to a major urban center. These geographical differences are reflected in the higher dust load and larger amounts of anthropogenic pollutants reaching this site. The local inhabitants of Waliguan are mainly sheep and yak herders, who cook and heat their tents using combustion of dry yak dung. This source of ammonia (NH<sub>3</sub>) is reflected in higher NH<sub>4</sub><sup>+</sup> concentrations measured at Waliguan despite lower concentrations of the other ionic constituents. At AS, the concentrations of SO<sub>4</sub><sup>2-</sup> and NO<sub>3</sub><sup>-</sup> were higher than those in Lhasa, Tibetan Autonomous Region, China, especially for SO<sub>4</sub><sup>2-</sup>, which is present at concentrations more than 10 times that in Lhasa. However, concentrations of Ca<sup>2+</sup> and Mg<sup>2+</sup> were very similar to those in Lhasa. The relatively higher concentrations of SO<sub>4</sub><sup>2-</sup> and NO<sub>3</sub><sup>-</sup> at BS reflect its proximity to Urumqi. The concentration of NO<sub>3</sub><sup>-</sup> at BS more than a factor of two lower than that measured in Germu and Xining, Qinghai Province and the mean values for northern China. Concentrations of Ca<sup>2+</sup> and Mg<sup>2+</sup> at BS were slightly lower than those in Germu and Xining, and higher than those in Lhasa. Germu and Xining are the two largest and most industrialized cities in Qinghai Province, so we expect a larger industrial impact than that observed at BS and

Lhasa. Sulfate was highest in samples collected at Urumqi, consistent with uncontrolled coal burning.

#### 4.4. Seasonal variability and possible reasons

The total ion loading (total water-soluble cations and anions measured) showed apparent seasonal variations both at BS and AS (Tables 4 and 5). However, the seasonality at these two stations showed quite different patterns.

The total ion loading reached maximum at AS during April and May when dust storms occurred frequently in the region. The concentrations reached a minimum during winter months (October–February) and remained relatively steady throughout the remaining months. The total ion load peaked during winter months (dry season) at BS. The ion load was also elevated during spring months and reached a minimum in summer. The seasonal variations of EC, pH, major ions and insoluble microparticles also confirmed this variation.

The interpretation of the different seasonal cycles observed at each measurement site is complex, likely relating to differences in both pollutant sources and vertical mixing. We present several hypotheses consistent with the measurements. When synoptic systems, specifically cold fronts, pass through this region, the resulting cloud often climbs upward from the basin along the valley prior to the onset of precipitation. According to Wang and Zhang (1985), this process increases the frequency of a valley wind. The contribution of the local convection does not make a large contribution to local precipitation, normally less than 10% of total annual precipitation.

Notable differences in the seasonal wind distributions at the two sites were observed. During both the wet season (from May to Sep.) and dry season, the most frequent wind direction was NNE at BS, but during the wet season the frequency of NNE wind was two times higher (Fig. 3). At AS the wind normally had an easterly component during the wet season and a westerly component during the dry season. The lack of a prominent valley wind during the dry season is reflected in increased atmospheric stability at AS.

At BS we found that maximum ion concentrations in precipitation occurred during periods of NNE and NE wind

**Table 3**  
Comparison of volume weighted mean chemical species of precipitation with those in northern China ( $\mu\text{eq. L}^{-1}$ ).

	BS	AS	Urumqi <sup>a</sup>	Waliguan <sup>b</sup>	Lhasa <sup>c</sup>	Germu and Xining <sup>d</sup>	Mean values of northern China <sup>b</sup>
Cl <sup>-</sup>	11.37	16.47	106.48	6.1	9.7	48.77	
SO <sub>4</sub> <sup>2-</sup>	63.86	52.97	297.92	24	5.2	84.01	197.1
NO <sub>3</sub> <sup>-</sup>	18.89	9.63	26.29	8.3	6.9	48.08	39.6
Na <sup>+</sup>	10.93	19.02	45.65	8.7	11.2	96.56	
NH <sub>4</sub> <sup>+</sup>	19.81	25.17	67.78	45.5	14.3	160.61	179.4
K <sup>+</sup>	5.3	4	18.97	3.8	5.14	69.17	
Mg <sup>2+</sup>	36.19	18.14	49.17	12.1	10.9	37.9	
Ca <sup>2+</sup>	257.27	174.19	239.5	34	197.4	314.31	317
pH	7.27	6.99	6.86	6.38	7.5	6.86	5.32
EC	35.51	26.98	91.04	14.58	25.6		

EC is  $\mu\text{s cm}^{-1}$ .

<sup>a</sup> Xu et al. (2007). Urumqi (43°50'N, 87°30'E, 800 m. a.s.l.).

<sup>b</sup> Tang et al. (2000). Waliguan (36°17'N, 100°54'E, 3816 m. a.s.l.).

<sup>c</sup> Zhang et al. (2003). Lhasa (29°30'N, 91°12'E, 3658 m. a.s.l.).

<sup>d</sup> Zhang et al. (2002). Germu (36°N, 94°E, 2500 m. a.s.l.) Xining (36°30'N, 101°21'E, 2800 m. a.s.l.).

**Table 4**Volume weighted mean ionic concentrations ( $\mu\text{eq. L}^{-1}$ ) and other species in precipitation at AS.

	Apr.-03	May-03	Jun.-03	Jul.-03	Aug.-03	Sep.-03	Oct.-03-Jan.-04	Feb.-04	Mean	Wet deposition flux	Dry deposition flux
Number	6	12	10	17	8	4	6	2			
Cl <sup>-</sup>	25.54	42.41	20.66	9.03	15.75	3.6	4.28	5.01	16.47	5.19	0.09
SO <sub>4</sub> <sup>2-</sup>	61.8	103.23	48.82	55.13	38.63	36.05	36.81	21.71	52.97	8.34	3.26
NO <sub>3</sub> <sup>-</sup>	8.59	20.06	10.56	7.21	8.51	3.56	15.94	5.36	9.63	3.03	0.18
Na <sup>+</sup>	32.68	57.84	20.63	13.44	12.27	6.85	6.34	5.89	19.02	5.99	2.49
NH <sub>4</sub> <sup>+</sup>	18.66	39.42	31.89	22.61	19.72	19.95	17.61	15.25	25.17	7.93	0.21
K <sup>+</sup>	5.49	7.21	3.18	3.31	3.3	10.7	3.68	1.98	4	1.26	0.48
Mg <sup>2+</sup>	37.52	62.17	22	8.11	11.09	10.22	18.57	12.42	18.14	2.86	1.5
Ca <sup>2+</sup>	253.98	493.66	160.95	125.6	119.78	222.61	112.36	103.21	174.19	27.43	8.6
pH	7.05	7.55	7.07	6.75	6.97	7.2	7.04	7.14	6.99		
EC	32.46	67.6	25.95	20.86	20.18	30.36	19.4	15.95	26.98		
Dust number	4.6	9.7	2.8	2.8	1.7	1.6	1.0	1.0	3.15		
Dust diameter	1.17	1.78	1.37	1.15	1.16	0.89	1.17	0.79	1.19		

The units of wet and dry deposition flux are  $\text{mmol m}^{-2} \text{yr}^{-1}$ ; EC is  $\mu\text{s cm}^{-1}$ ; dust number is  $1 \times 10^5 \text{ ml}^{-1}$ ; dust diameter is  $\mu\text{m}$ , the unit of deposition flux is  $\text{mmol m}^{-2} \text{yr}^{-1}$ .

regimes (valley wind direction) and also during periods with relatively high wind velocities ( $>4 \text{ m s}^{-1}$ ). This suggests that pollutants and local dust from Urumqi and Houxia contributed to the peak concentrations of ions in the measured precipitation. The same phenomenon was also found by Li et al. (2006). At AS some peak values did not correspond to ENE or NE (valley wind), but did occur during periods with elevated wind speeds.

A significant portion of the high wintertime ion loading at BS can be explained, by the presence of a strong inversion layer. A study in the Urumqi River basin (Zhang et al., 1994) identified a strong inversion layer between 1000 and 2400 m from November to March. This persistent inversion layer traps local air pollution. The inversion layer was present during the most serious air pollution event in Urumqi city, which occurred from 16 December 2003 to 11 January 2004 (Guo et al., 2006). In contrast, AS is rarely influenced by an inversion layer, and consequently the minimum ion loading occurred during winter at this site.

The other major factor impacting BS is emissions from coal combustion during home and factory heating, which is considerable during winter months. This region is sufficiently cold so domestic and industrial heating occurs October 15–April 15. Seasonal local coal combustion is also responsible for seasonal patterns in particulate matter in

this region. Bi et al. (2007) pointed out that PM<sub>10</sub> in Urumqi city reached maximum in winter (dry season) and a minimum in summer. During winter months coal combustion fly ash accounted for 59% of PM<sub>10</sub>, compared to 15% during summer months. The same pattern was observed at BS.

#### 4.5. Dust storm events

We expect the largest impact from dust to occur during the months of April and May because this is when airborne dust is most abundant throughout our study area. We routinely observed the maximum ion concentration of Ca<sup>2+</sup>, a major component of soil dust, when dust events were also observed from several Satellite platforms (<http://dear.cma.gov.cn>), including FY-1D and FY-10 (China Meteorological Administration) and NOAA-16.

The observed precipitation chemistry during dust storm events are provided in Table 6. The peak ion concentrations in precipitation on 20 April 2003 at AS, 18 April and 22 April at BS were preceded by dust events that started on 16–17 April in this region. Dust events observed 11–14 May were followed by elevated ion concentrations on 18 May and 21 May at AS and BS, respectively. We identified two other dust events (2 May and 26 May) that did not impact

**Table 5**Volume weighted mean ionic concentrations ( $\mu\text{eq. L}^{-1}$ ) and other species in precipitation at BS.

	Apr.- 03	May-03	Jun.-03	Jul.-03	Aug.-03	Sep.-03	Oct. 03-Jan. 04	Feb. 04	Mean	Wet deposition flux	
Number	4	9	13	16	11	3	3	4			
Cl <sup>-</sup>	11	13.97	13.18	6.46	13.03	20.69	27.68	10.45	11.37	4.06	
SO <sub>4</sub> <sup>2-</sup>	58.42	96.24	55.48	42.64	56.76	81.83	184.19	237.21	63.86	11.41	
NO <sub>3</sub> <sup>-</sup>	12.48	22.83	24.84	19.32	12.38	16.38	6.42	13.47	18.89	6.75	
Na <sup>+</sup>	11.54	16.93	11.24	5.25	12.2	20.01	28.62	15.62	10.93	3.91	
NH <sub>4</sub> <sup>+</sup>	16.52	23.89	20.5	16.62	24	21.65	9.81	6.35	19.81	7.08	
K <sup>+</sup>	7.55	7.23	4.29	3.08	6.16	9.93	14.39	10.68	5.3	1.89	
Mg <sup>2+</sup>	38.39	45.91	31.06	22.9	36.74	44.78	142.22	150.55	36.19	6.47	
Ca <sup>2+</sup>	576.71	365.67	219.98	161.62	199.79	311.39	909.6	1185.56	257.27	45.99	
pH	7.5	7.41	7.19	7.15	7.26	7.49	7.93	8.09	7.27		
EC	55.58	44.91	32.1	24.43	32.83	46.65	112.99	133.69	35.51		
Dust number	3.7	3.8	2.4	0.9	2.4	2.8	2.2	3.5	2.7		
Dust diameter	1.35	1.19	2.0	1.0	1.17	1.0	1.06	1.93	1.34		

The units of wet and dry deposition flux are  $\text{mmol m}^{-2} \text{yr}^{-1}$ ; EC is  $\mu\text{s cm}^{-1}$ ; dust number is  $1 \times 10^5 \text{ ml}^{-1}$ ; dust diameter is  $\mu\text{m}$ , the unit of deposition flux is  $\text{mmol m}^{-2} \text{yr}^{-1}$ .

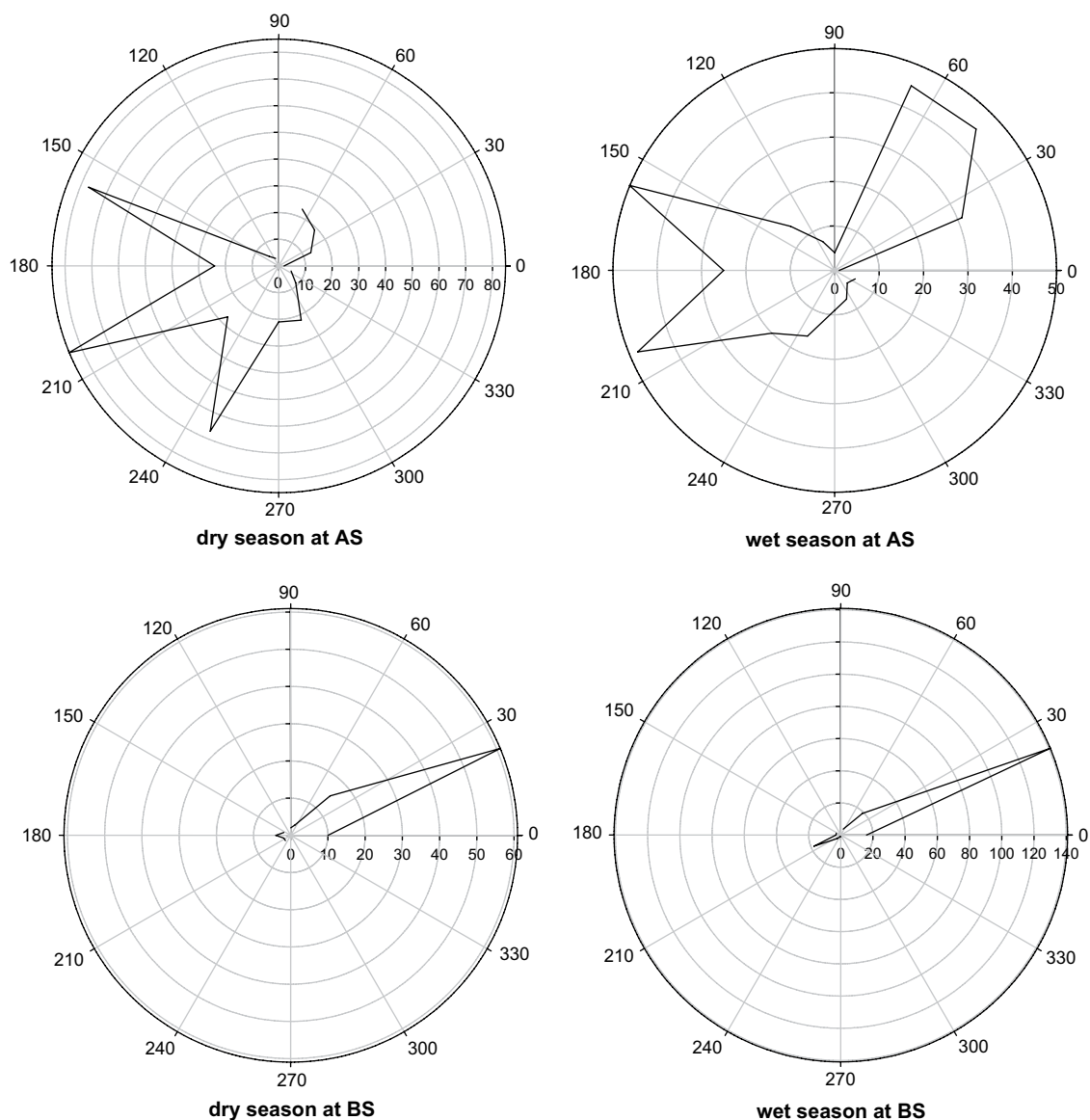


Fig. 3. Wind direction in dry and wet season at AS and BS.

precipitation at BS. Satellite images indicated that these dust events originated in the Taklimakan Desert. Those plumes climbed up the Tien Shan, traveled at a higher elevation than other events originating outside of the Taklimakan basin. These particular events did influence AS, but an impact at BS was not identified. During this period the total ion loading at AS was much higher than that at BS. The precipitation samples collected during the Taklimakan dust storms also had more insoluble particles and the particles had a larger mean diameter compared to the mean diameter ( $1.33 \mu\text{m}$ ) and number ( $2.3 \times 10^5 \text{ ml}^{-1}$ ) of insoluble microparticles measured during the other dust storm events. Based on our analysis, we believe that the concentration of insoluble particles in precipitation can be used to infer the intensity and frequency of dust events in this region.

#### 4.6. Origins of major ionic species

We calculated correlation coefficients between the various chemical species measured in the precipitation samples. These correlation coefficients can be used to identify and separate the impact of various sources influencing the chemical composition of the precipitation.

Mineral particles originating in the Taklimakan Desert of western China are composed primarily of  $\text{Na}^+$ ,  $\text{Mg}^{2+}$ ,  $\text{Cl}^-$  and  $\text{Ca}^{2+}$  (Okada and Kai, 2004).  $\text{Ca}^{2+}$  in mineral particles is present in two forms: 1) as  $\text{CaCO}_3$ , and 2)  $\text{CaSO}_4$  also as an internal mixture of  $\text{CaCO}_3$  and  $\text{CaSO}_4$  (Hseung and Jackson, 1952; Okada and Kai, 1995).

We found (Tables 7 and 8) that  $\text{Mg}^{2+}$  was highly correlated with  $\text{Ca}^{2+}$  ( $R = 0.892$  at BS and  $R = 0.883$  at AS), as well as with  $\text{SO}_4^{2-}$  ( $R = 0.813$  at BS and  $R = 0.594$  at AS).

**Table 6**Chemical species ( $\mu\text{eq. L}^{-1}$ ) in special precipitation samples during dust storm periods.

	$\text{Cl}^-$	$\text{SO}_4^{2-}$	$\text{NO}_3^-$	$\text{Na}^+$	$\text{NH}_4^+$	$\text{K}^+$	$\text{Mg}^{2+}$	$\text{Ca}^{2+}$	pH	EC	Dust number	Diameter
20 Apr. (AS)	71.65	413.6	nd	137.97	22.55	7.19	131.65	800.4			6.5	0.94
2 May (AS)	94.11	159.58	17.18	114.25	41.7	8.15	84.75	544.3	7.67	82.9	4.6	2.88
18 May (AS)	266.73	264.0	56.53	261.5	120.89	9.0	125.86	1151	7.75	160.6	29.7	2.29
31 May (AS)	134.73	169.13	16.13	132.86	16.14	5.08	103.46	842	7.85	110.3	32.1	1.88
18 Apr. (BS)	4.52	101.56	16.55	9.39	11.12	8.71	59.72	928				
22 Apr. (BS)	29.7	53.5	12.63	26.88	20.71	21.29	65.1	1162	8.2	126.8	4.7	1.73
21 May (BS)	27.22	250.12	51.86	51.09	68.54	20.49	98.33	739				

EC is  $\mu\text{s cm}^{-1}$ ; dust number is  $1 \times 10^5 \text{ ml}^{-1}$ ; dust diameter is  $\mu\text{m}$ .

$\text{Ca}^{2+}$  was also highly correlated with  $\text{SO}_4^{2-}$  ( $R = 0.851$  at BS and  $R = 0.645$  at AS). The strong relationship between  $\text{Ca}^{2+}$ ,  $\text{Mg}^{2+}$  and  $\text{SO}_4^{2-}$  at BS suggested that local coal pollution heavily influences the precipitation chemistry at this site. Bi et al. (2007) concluded that coal combustion could be a source for each of these species. The cement plant is also likely an additional source of  $\text{Ca}^{2+}$ ,  $\text{Mg}^{2+}$  and  $\text{SO}_4^{2-}$  at BS. In addition to being a major component of soil dust,  $\text{Ca}^{2+}$  is also a major component of fly ash. Thus, we can believe that a substantial portion of the  $\text{Ca}^{2+}$  observed in samples collected at BS can be traced to fly ash from local coal use.

The strong relationship between  $\text{Na}^+$  and  $\text{Cl}^-$  ( $R = 0.942$  and  $R = 0.891$  for BS and AS, respectively) indicate that they likely have a similar source. Wake et al. (1990) inferred that  $\text{Na}^+$  and  $\text{Cl}^-$  in the Tien Shan likely reflect an input of  $\text{Na}^+$  and  $\text{Cl}^-$  from evaporation in areas to the north of the Tien Shan. Halite ( $\text{NaCl}$ ) is also an important component of the sand in the Taklamakan desert and Southwest Tien Shan (Okada and Kai, 2004).

$\text{NO}_3^-$  in precipitation tends to be highest in regions with significant nitrogen oxides ( $\text{NO}_x$ ). Neither AS or BS are located in densely populated areas with numerous vehicles. Consequently the  $\text{NO}_3^-$  measured in the precipitation samples was relatively low. As expected, the concentration of  $\text{NO}_3^-$  was higher at BS due to its closer proximity to the industrial area.  $\text{NH}_4^+$  in precipitation results from the incorporation of  $\text{NH}_3$  and particles containing  $\text{NH}_4^+$  into both clouds and rainwater. Major local sources of  $\text{NH}_3$  include bacterial decomposition of urea in animal excreta, emissions from natural or fertilized soils, and domestic fuel wood combustion.

The Waliguan station, located at the northeastern part of the Tibetan Plateau, is a land-based Global Atmospheric Watch (GAW) base station, which has been shown to be minimally impacted by dust and local sources of pollution and is representative of “background” conditions in the

Northwestern China (Tang et al., 2000). If we accept an assumption that Waliguan is representative of background conditions, we can compare samples from AS to the “background” condition and calculate approximately what portion of the ions observed in the precipitation at AS are due to anthropogenic pollution and dust storm. We can write the anthropogenic percent contribution at AS as  $(X_{\text{AS}} - X_{\text{Waliguan}})/X_{\text{AS}} \times 100\%$  where  $X$  indicates the volume-weighted mean concentration of ions in precipitation.

Based on this approximation, the contribution of anthropogenic activities and dust to the ionic concentrations of  $\text{Ca}^{2+}$ ,  $\text{Mg}^{2+}$ ,  $\text{SO}_4^{2-}$  and  $\text{NO}_3^-$  at AS are about 80.5, 33.3, 54.7, and 13.8%, respectively. This estimate suggests that although mineral aerosol sources are the major contributor to the total precipitation content at AS, anthropogenic activities also have some impact.

#### 4.7. Wet deposition and dry deposition

Thus far we have only discussed wet deposition of water soluble species, which occurs mainly during the months of May to September. Deposition of these species during the remaining months can be estimated using the observed mean aerosol concentration and calculated deposition velocities. Deposition velocities vary with aerosol particle size but are not well constrained (Duce et al., 1991). Fine and coarse fractions were not determined during this study, but we make several assumptions to allow us to coarsely estimate deposition fluxes during the dry season. We assume that crustal components  $\text{Ca}^{2+}$ ,  $\text{Mg}^{2+}$ ,  $\text{K}^+$  and  $\text{Na}^+$  (based on enrichment factors, Bridges, 1998) are predominantly associated with coarse mode aerosol and have dry deposition velocities of  $2 \text{ cm s}^{-1}$  while all other species are associated with fine mode aerosol and have dry deposition velocities of  $0.1 \text{ cm s}^{-1}$  (Duce et al., 1991). Based on the work of Duce et al. (1991) we expect that these

**Table 7**The correlation matrix for the species in precipitation at AS ( $N = 65$ ,  $p \leq 0.05$ ).

	$\text{Cl}^-$	$\text{SO}_4^{2-}$	$\text{NO}_3^-$	$\text{Na}^+$	$\text{NH}_4^+$	$\text{K}^+$	$\text{Mg}^{2+}$	$\text{Ca}^{2+}$	pH
$\text{Cl}^-$									
$\text{SO}_4^{2-}$	0.643								
$\text{NO}_3^-$	0.417	0.53							
$\text{Na}^+$	0.891	0.775	0.432						
$\text{NH}_4^+$	0.519	0.43	0.323	0.51					
$\text{K}^+$	0.277	0.462	0.215	0.338	0.329				
$\text{Mg}^{2+}$	0.745	0.594	0.451	0.716	0.269	0.329			
$\text{Ca}^{2+}$	0.738	0.645	0.417	0.697	0.222	0.502	0.883		
pH	0.439	0.445	0.263	0.434	0.26	0.522	0.743	0.803	

**Table 8**

The correlation matrix for the species in precipitation at BS ( $N=63$ ,  $p \leq 0.05$ ).

	Cl <sup>-</sup>	SO <sub>4</sub> <sup>2-</sup>	NO <sub>3</sub> <sup>-</sup>	Na <sup>+</sup>	NH <sub>4</sub> <sup>+</sup>	K <sup>+</sup>	Mg <sup>2+</sup>	Ca <sup>2+</sup>	pH
Cl <sup>-</sup>									
SO <sub>4</sub> <sup>2-</sup>	0.388								
NO <sub>3</sub> <sup>-</sup>	0.264	0.477							
Na <sup>+</sup>	0.942	0.536	0.397						
NH <sub>4</sub> <sup>+</sup>	0.266	0.083	-0.072	0.194					
K <sup>+</sup>	0.604	0.579	0.27	0.777	0.302				
Mg <sup>2+</sup>	0.41	0.813	0.281	0.542	-0.197	0.469			
Ca <sup>2+</sup>	0.319	0.851	0.351	0.475	-0.2	0.518	0.892		
pH	0.406	0.709	0.116	0.522	-0.108	0.545	0.825	0.893	

assumed values for deposition velocities could vary from the actual values by a factor of 3. Another source of error comes from our assumption that SO<sub>4</sub><sup>2-</sup> is primarily in the fine mode. SO<sub>4</sub><sup>2-</sup> may also be associated with coarse mode particles due to displacement reactions with mineral dust. We also recognize that gypsum could make up a significant fraction of the coarse mode dust particles, and this possibility also weakens our assumption that all the sulfate is in the fine mode. Because of the uncertainties in our assumptions, all estimates of dry deposition are only reported to one significant figure.

The deposition velocities that we assume are consistent with those used by Zhang et al. (1998) under similar conditions in northern China. Here we use the average aerosol concentrations to approximately calculate the yearly dry deposition fluxes. To estimate wet deposition fluxes, volume-weighted averaged concentrations were calculated and multiplied by the total precipitation amount for the year (Bridges, 1998).

Annual dry and wet deposition fluxes of ionic species are also shown in Tables 4 and 5 and Fig. 4. At AS the total deposition of all species is dominated by wet deposition. The dry deposition flux of Ca<sup>2+</sup>, Mg<sup>2+</sup>, K<sup>+</sup>, Na<sup>+</sup> and SO<sub>4</sub><sup>2-</sup> comprised 24, 34, 28, 28, and 29% of the total flux, respectively. NH<sub>4</sub><sup>+</sup>, NO<sub>3</sub><sup>-</sup> and Cl<sup>-</sup> accounted for less than 6% of the total flux. Our crude estimates indicate that the dry deposition of Ca<sup>2+</sup>, Mg<sup>2+</sup>, K<sup>+</sup>, Na<sup>+</sup> and SO<sub>4</sub><sup>2-</sup> are important at this site, contributing approximately a third of the total flux. This does not seem to be the case for NH<sub>4</sub><sup>+</sup>, NO<sub>3</sub><sup>-</sup> and Cl<sup>-</sup>, where based

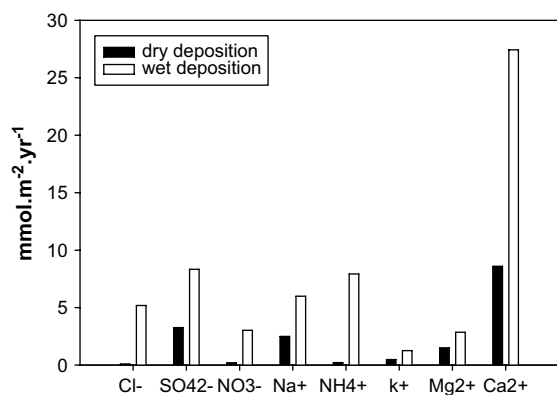


**Fig. 4.** Comparison of annual dry and wet deposition fluxes of ionic species at AS.

on our estimates, dry deposition makes up a smaller portion of the total deposition flux. We recognize that this flux may not be insignificant for the impacted ecosystems, just minor in terms of the total flux.

Compared with values in Beijing, Jinan, and Nanjing in east China, the wet deposition level of major ions at AS were quite low. However, these values are higher than those reported for the Korean peninsula, Japan and throughout Asia (Lee et al., 2000). With the exception of Ca<sup>2+</sup> and Mg<sup>2+</sup>, the wet deposition of the major ions at BS was lower than that reported for Beijing, Jinan, and Nanjing. Wet depositions of Ca<sup>2+</sup> and Mg<sup>2+</sup> at BS were very similar to values reported for these cities.

## 5. Conclusion

An investigation of precipitation chemistry was carried out in the Urumqi River Valley, eastern Tien Shan, China during the period of April 2003–February 2004. The results showed that Ca<sup>2+</sup> was the dominant cation, and SO<sub>4</sub><sup>2-</sup> was the dominant anion in this region. Seasonal variations can be explained by both meteorological and anthropogenic factors. Asian mineral aerosol sources were the main contributor to the total precipitation content at this region, and reached a maximum contribution during spring months. Although BS can be classified as a rural site, it was affected by coal combustion in nearby population centers, especially during winter months when the region is under the influence of a strong inversion layer.

Calculated wet and dry deposition fluxes suggest that dry deposition of Ca<sup>2+</sup>, Mg<sup>2+</sup>, K<sup>+</sup>, Na<sup>+</sup> and SO<sub>4</sub><sup>2-</sup> is comparable to the wet deposition of these species. This is not the case for NH<sub>4</sub><sup>+</sup>, NO<sub>3</sub><sup>-</sup> and Cl<sup>-</sup>, where wet deposition clearly dominates.

This study has provided important insight into seasonal variations in precipitation chemistry and deposition fluxes at two sites in the eastern Tien Shan; however, other monitoring sites would be necessary to determine whether these results are representative of the surrounding region. Continued studies on precipitation chemistry with more extensive spatial and temporal coverage are necessary to better understand the issues discussed here.

## Acknowledgements

This research was supported by the National Natural Science Foundation of China (J0630966; 40571033; 40631001). We would like to thank two anonymous reviewers, who have contributed valuable comments to improving the manuscript. Also we would thank Zhu Yuman for chemical analysis.

## References

- Bi, X.H., Feng, Y.C., Wu, J.H., Wang, Y.Q., ZHU, T., 2007. Source apportionment of PM<sub>10</sub> in six cities of northern China. *Atmospheric Environment* 41, 903–912.
- Bridges, K., 1998. Deposition processes and their impact on a heavily industrialised region of the Northern Czech Republic. Unpublished Ph.D. thesis, University of East Anglia, UK.
- Duce, R.A., et al., 1991. The atmospheric input of trace species to the world ocean. *Global Geochemical Cycles* 5 (3), 193–259.

- Guo, Y.H., Gao, L.J., Li, A.H., 2006. Analysis of a most serious air pollution at winter in Urumqi. *Environmental Chemistry* 25 (3), 379–380 (in Chinese).
- Hseung, Y., Jackson, M.L., 1952. Mineral composition of the clay fraction of some main soil groups of China. *Soil Science Society of American Proceedings* 16, 97–110.
- Jiang, F., Zhu, C., Wei, W., Abe, O., 2002. Some results of chemical surveys in the Kunnes River valley, East Tianshan mountains, China. *Atmospheric Environment* 36, 4941–4949.
- Lee, B.K., Hong, S.H., Lee, D.S., 2000. Chemical composition of precipitation and wet deposition of major ions on the Korean peninsula. *Atmospheric Environment* 34, 563–575.
- Lee, X., Qin, D., Jiang, G., Duan, K., Zhou, H., 2003. Atmospheric pollution of a remote area of Tianshan Mountain: ice core record. *Journal of Geophysical Research* 108 (D14), 4406–4416.
- Li, J., Zhuang, G.S., Huang, K., Lin, Y.F., Xu, C., Yu, S.L., 2007. Characteristics and sources of air-borne particulate in Urumqi, China, the upstream area of Asia dust. *Atmospheric Environment*. doi:10.1016/j.atmosenv.2007.09.062.
- Li, Z.Q., Ross, E., Thompson, E.M., Wang, F.T., Dong, Z.B., You, X.N., Li, H.L., Li, C.J., Zhu, Y.M., 2006. Seasonal variability of ionic concentrations in surface snow and elution processes in snow-firn packs at the PGPI site on Glacier No. 1 in eastern Tianshan, China. *Annals of Glaciology* 43, 250–256.
- Liu, B.Y.H., Pui, D.Y.H., Rubow, K.L., 1984. Characteristics of air sampling filter media. In: Marple, V.A., Liu, B.Y.U. (Eds.), *Aerosols in the Mining and Industrial Work Environments. Instrumentation*, vol. 3. Ann Arbor Science, MI, pp. 989–1037.
- Mamtimin, B., Meixner, F.X., 2007. The characteristics of air pollution in the semi-arid city of Urumqi (NW China) and its relation to climatological process. *Geophysical Research Abstracts* 9, 06357.
- Momin, G.A., Ali, K., Rao, P., Safai, P., Chate, D., Praveen, 2005. Study of chemical composition of rainwater at an urban (Pune) and a rural (Sinhagad) location in India. *Journal of Geophysical Research* 110. doi:10.1029/2004JD004789 D08302.
- Okada, K., Kai, K., 1995. Features and elemental composition of mineral particles collected in Zangye, China. *Journal of Meteorological Society of Japan* 73, 947–957.
- Okada, K., Kai, K., 2004. Atmospheric mineral particles collected at Qira in the Taklamakan Desert, China. *Atmospheric Environment* 38, 6927–6935.
- Parashar, D.C., et al., 1996. A Preliminary Report on an Indo-Swedish Project on Atmospheric Chemistry. Report CM 90. Department of Meteorology, Stockholm University, Stockholm.
- Sun, J.Y., Qin, D.H., Mayewski, P.A., Dibb, J.E., Whitlow, S., Li, Z.Q., Yang, Q.Z., 1998. Soluble species in aerosol and snow and their relationship at Glacier No.1, Tien Shan, China. *Journal of Geophysical Research* 103 (D21), 28021–28028.
- Tang, J., Xue, H.S., Yu, X.L., Cheng, H.B., Xu, X.B., Zhang, X.C., Ji, J., 2000. The preliminary study on chemical characteristics of precipitation at Mt. Waliguan. *Acta Science Circumstance* 20 (4), 420–425 (in Chinese).
- Tiwari, S., Kulshrestha, U.C., Padmanabhamurty, B., 2007. Monsoon rain chemistry and source apportionment using receptor modeling in and around National Capital Region(NCR) of Delhi, India. *Atmospheric Environment* 41, 5595–5604.
- Wake, C.P., Mayewski, P.A., Spencer, M.J., 1990. A review of central Asia glaciochemical data. *Annals of Glaciology* 14, 301–306.
- Wake, C.P., Mayewski, P.A., Ping, Wang, Qinzhao, Yang, Jiankang, Han, Zichu, Xie, 1992. Anthropogenic sulfate and Asia dust signals in snow from Tien Shan, Northwest China. *Annals of Glaciology* 16, 45–52.
- Wang, D., Zhang, P., 1985. Climate in Urumqi River valley Tianshan. *Journal of Glaciology and Geocryology* 7, 239–247 (in Chinese).
- Williams, M.W., Tonnessen, K.A., Melack, J.M., Yang, Daqing, 1992. Sources and spatial variation of the chemical composition of snow in the Tien Shan, China. *Annals of Glaciology* 16, 25–32.
- Xu, M., Lu, A.H., Xu, F., Wang, B., 2007. Seasonal chemical composition variations of wet deposition in Urumchi, Northwestern China. *Atmospheric Environment*. doi:10.1016/j.atmosenv.2007.11.008.
- Zhang, D.D., Peart, M.R., Jim, C.Y., 2002. Alkaline rains on the Tibetan Plateau and their implication for the original pH of natural rainfall. *Journal of Geophysical Research* 107 (D14). doi:10.1029/2001JD001332.
- Zhang, D.D., Peart, M.R., Jim, C.Y., He, Y.Q., Li, B.S., Chen, J.A., 2003. Precipitation chemistry of Lhasa and other remote towns, Tibet. *Atmospheric Environment* 37, 231–240.
- Zhang, X.Y., Arimoto, R., Zhu, G.H., Chen, T., Zhang, G.Y., 1998. Concentration, size distribution and deposition of mineral aerosol over Chinese desert regions. *Tellus* 50 (B), 317–330.
- Zhang, Y., Kang, E., Liu, C., 1994. Mountain climate analysis in Urumqi River valley, Tianshan. *Journal of Glaciology and Geocryology* 16 (4), 333–341 (in Chinese).
- Zhao, Z., Li, Z., 2004. Determination of soluble ions in atmospheric aerosol by ion chromatography. *Modern Science Instrument* 5, 46–49 (in Chinese).
- Zhao, Z.P., Li, Z.Q., Ross, E., Wang, F.T., Li, H.L., Zhu, Y.M., 2006. Atmosphere-to-snow-to-firn transfer of  $\text{NO}_3^-$  on Glacier No. 1, eastern Tien Shan, China. *Annals of Glaciology* 43, 239–244.